

Thermalization of gluons at RHIC: Dependence on initial conditions

Zhe Xu¹ and Carsten Greiner¹

¹ Institut für Theoretische Physik, Johann Wolfgang Goethe Universität Frankfurt, Max-von-Laue Str. 1, D-60438 Frankfurt, Germany

Received

Abstract. We investigate how thermalization of gluons depends on the initial conditions assumed in ultrarelativistic heavy ion collisions at RHIC. The study is based on simulations employing the pQCD inspired parton cascade solving the Boltzmann equation for gluons. We consider independently produced minijets with $p_T > p_0 = 1.3 \sim 2.0$ GeV and a color glass condensate as possible initial conditions for the freed gluons. It turns out that full kinetic equilibrium is achieved slightly sooner in denser system and its timescale tends to saturate. Compared with the kinetic equilibration we find a stronger dependence of chemical equilibration on the initial conditions.

Keywords: thermalization, heavy ion collisions, Monte Carlo simulations

PACS: 05.60.-k, 24.10.Lx, 25.75.-q

1. Introduction

Recently we have studied kinetic and chemical equilibration of gluons in a central heavy ion collision at RHIC energy employing a microscopical transport model including multiple $gg \leftrightarrow ggg$ scatterings [1]. The results showed that even for an initially dilute system, $dN_g/dy \approx 200$, when the initial conditions are assumed as independent minijets with $p_T > p_0 = 2.0$ GeV, overall kinetic equilibrium is achieved at 2 fm/c and full chemical equilibrium follows later at about 3 fm/c. In addition, the expansion of the considered parton system behaves (quasi)hydrodynamically. Especially the total transverse energy per unit rapidity at midrapidity, $dE_T/dy|_{y=0}$, decreases from initial 500 GeV to 270 GeV at final time 4 fm/c due to the longitudinal work done by the pressure built up during the thermal equilibration.

Since the experiments at RHIC at $\sqrt{s} = 200$ GeV obtained $dE_T/dy|_{y=0} = 620 \pm 33$ GeV [2] for the 5% most central events, our final value is lower by a

factor of more than two when assuming that hadronization does not change the local energy density. The cutoff $p_0 = 2$ GeV used in the simulations has been a rather conservative assumption for the initial minijets. *Soft* partons with $p_T < p_0$, which are produced by the nonperturbative part of nucleus-nucleus interaction and also contribute to the entropy production, are completely neglected. Such partons may stem from the color glass condensate (CGC) [3] and should also be included in the transport simulation, when they are freed from the color field. In principle, one should combine gluons from CGC and harder gluons from minijets production to give a more realistic initial condition for partons after a heavy ion collision. The final results after parton evolution with such initial condition is thus appropriate for comparisons with the experimental data. We leave this interesting topic for future investigations. For the moment, initial conditions of gluons from CGC and minijets production are assumed separately for independent simulations.

In another idea within a saturation picture of quarks and gluons in phase space, presented by Eskola et al. [4], the authors assumed that performing the computation of minijets at a saturation momentum, $p_0 = p_{sat}$, gives an estimate of the effect from all momentum scales, both above and below p_{sat} . At RHIC energy they got $p_{sat} = 1.13$ GeV for corresponding initial minijets, and estimated the final transverse energy $dE_T/dy|_{y=0} \approx 660$ GeV by assuming *immediate* thermalization and adiabatic expansion. Compared with the experimental data, the calculations met the value of the transverse energy. The smaller the cutoff p_0 is assumed, the larger will be the initial gluon density. Intuitively, a denser system may achieve faster thermalization than a dilute system. However, immediate thermalization might be a naive assumption, particularly for chemical equilibration. This strongly motivates us to apply the developed parton cascade to inspect the timescale of thermalization in dependence on the cutoff parameter p_0 .

2. Initial Conditions

The production of the primary partons at the very onset of a central Au Au collision is assumed first as a free superposition of minijets being liberated in the individual semihard nucleon-nucleon interactions. We introduce an additional *formation time* for every minijet, $\Delta t_f = \cosh y \Delta \tau_f \approx \cosh y \cdot 1/p_T$, which models the prior off-shell propagation of the to be freed, on-shell partons in the scattering process. Within that time span, one assumes, for simplicity, that the still virtual parton does not interact and moves with speed of light. The p_0 dependence of initial conditions is shown in Table 1. The calculations are performed by multiplying the number of individual nucleon-nucleon collisions for a Au Au collision and the number of gluons produced in a nucleon-nucleon collision at $\sqrt{s} = 200$ GeV. The former is obtained by applying a Glauber picture with a Woods-Saxon nuclear distribution. The latter is evaluated employing the Glück-Reya-Vogt parametrizations [5] for the parton structure functions. One sees that the initial gluon number and transverse energy increase with decreasing p_0 .

Table 1. Gluon number and transverse energy per unit rapidity at midrapidity extracted from different initial conditions and at final time 4 fm/c after cascade simulations.

p_0/Q_s [GeV]	$\frac{dN_g}{dy}$ (init.)	$\frac{dN_g}{dy}$ (4 fm/c)	$\frac{dE_T}{dy}$ (init.)	$\frac{dE_T}{dy}$ (4 fm/c)
			[GeV]	[GeV]
$p_0 = 2.0$	181	352	478	272
$p_0 = 1.5$	537	663	1082	514
$p_0 = 1.4$	688	781	1301	626
$p_0 = 1.3$	889	930	1569	775
$Q_s = 1.0$	830	528	550	314

For the initial gluon distribution from the saturation picture we employ an idealized and boost-invariant form proposed by Mueller [6] and express it as

$$f(x, p) = \frac{c}{\alpha_s N_c} \frac{1}{\tau_f} \delta(p_z) \Theta(Q_s^2 - p_T^2), \quad (1)$$

which is described by a bulk scale Q_s , the momentum scale at which gluon distribution saturates. Distribution (1) has been used in [7] to investigate kinetic equilibration of gluons in the subsequent evolution by means of a non-linear Landau equation. In contrast to the minijets the saturation model gives the distribution of partons with $p_T < Q_s$. We read off the value of parameters taken in [7]: $N_c = 3$ for SU(3), $c = 1.3$, $\alpha_s = 0.3$, $Q_s = 1$ GeV and the corresponding formation time, at which gluons become on-shell, to be $\tau_f = 0.4$ fm/c $\sim 1/Q_s$, and assume that gluons will be produced within a transverse radius of 6 fm (Au nucleus). Then we obtain $dN_g/dy|_{y=0} = 830$ and $dE_T/dy|_{y=0} = 550$ GeV, which are also included in Table 1 for comparisons.

3. Setup for transport simulations

The three-body gluonic interactions are described by the matrix element [8]

$$|\mathcal{M}_{gg \rightarrow ggg}|^2 = \left(\frac{9g^4}{2} \frac{s^2}{(\mathbf{q}_\perp^2 + m_D^2)^2} \right) \left(\frac{12g^2 \mathbf{q}_\perp^2}{\mathbf{k}_\perp^2 [(\mathbf{k}_\perp - \mathbf{q}_\perp)^2 + m_D^2]} \right) \Theta(k_\perp \Lambda_g - \cosh y), \quad (2)$$

where $g^2 = 4\pi\alpha_s$. \mathbf{q}_\perp and \mathbf{k}_\perp denote, respectively, the perpendicular component of the momentum transfer and that of the momentum of the radiated gluon in the c.m. frame of the collision. We regularize the infrared divergences by using the Debye screening mass m_D^2 which is calculated locally over the present particle density obtained from the simulation. The suppression of the radiation of soft gluons due to the Landau-Pomeranchuk-Migdal (LPM) effect, which is expressed via the step function in Eq. (2), is modeled by the consideration that the time of the emission,

$\sim \frac{1}{k_\perp} \cosh y$, should be smaller than the time interval between two scatterings or equivalently the gluon mean free path Λ_g . This leads to a lower cutoff of k_\perp and to a decrease of the total cross section. The dependence of the total cross section on the LPM-cutoff is approximately logarithmic and thus its sensitivity to the dynamics is only moderate.

Comparing to the default setup in [1] two improvements are made concerning local incorporation of the screening mass and the transverse flow. In order to calculate the screening mass in a local region more accurately, we make use of the spherical symmetry in central collision and divide transverse plan in each Δz -bin into rings: from center to outer the first ring has a region of $0 < x_T < 1.5$ fm (x_T being the transverse radius), and the next rings have a width of 1 fm in transverse radius. The rings are regarded as local region where the screening mass will be evaluated.

Secondly, as implemented in [1], local collision rates of all interaction channels, which will be applied to model the LPM effect, are evaluated in individual cells. This leads to large fluctuations in the mean free path in those cells with small number of test particles. In order to reduce these fluctuations, we take the averaged value of collision rates over all the cells within individual rings. In addition, transverse velocities of rings are taken into account for calculating the collision rates.

4. Results

The space time propagations of gluons are simulated until a final time 4 fm/c at which the energy density at midrapidity at $p_0 = 2.0$ GeV has already decreased nearly to the critical value of 1 GeV/fm³ being characteristic for hadronization. The gluon number and transverse energy per rapidity at the final time are shown in Table 1. Comparing with the initial values the enhancement of gluon number is weaker at smaller p_0 , which implies larger initial fugacity at smaller p_0 . On the contrary, the initial gluons from the saturation model are, surprisingly, *oversaturated*. This can be interpreted as follows. According to the gluon distribution (1) the initial effective temperature is $T(\tau_f) = \epsilon/3n = 2/9 * Q_s$. We obtain then the effective gluon fugacity at the formation time

$$\lambda_g(\tau_f) = \frac{n}{n_{eq}} = \frac{\frac{dN}{\pi R^2 \tau_f d\eta}}{2(N_c^2 - 1) \frac{T^3}{\pi^2}} = \frac{9^3}{4^3} \frac{c}{\alpha_s N_c \tau_f Q_s}, \quad (3)$$

which would be valid when assuming immediate kinetic equilibrium at $\tau = \tau_f$. For the setup of parameters given before one has $\lambda_g(\tau_f) = 8$! So after the gluons are freed from the color field and become on-shell, $ggg \rightarrow gg$ collisions will be the dominant processes driving the system into chemical equilibrium.

From Table 1 one also sees that in all cases of initial conditions the transverse energy per unit rapidity decreases with the progressing time due to the onset of collective expansion. The final values of $dE_T/dy|_{y=0}$ are, however, quite different. We see that the value at $p_0 = 1.4$ GeV would meet the experimental data. Thus the

minijets production at $p_0 = 1.4$ GeV seems to give an appropriate initial condition of gluons at RHIC. To show the decreasing of the transverse energy at midrapidity we depict in Fig. 1 the normalized transverse energies obtained from simulations with the different initial conditions. The denominators are the transverse energies

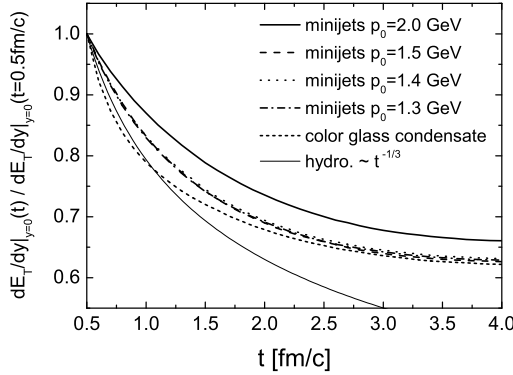


Fig. 1. Time evolution of normalized transverse energy per unit rapidity at midrapidity. Results are obtained from simulations with different initial conditions of gluons, assumed in a central Au Au collision at RHIC energy.

at midrapidity at time 0.5 fm/c, which are nearly the initial values shown in Table 1. We see a unique behavior of the time evolutions of the normalized $dE_T/dy|_{y=0}$, especially for initial conditions employing minijets with $p_0 = 1.3 - 1.5$ GeV and CGC with $Q_s = 1.0$ GeV. For these initial conditions the decreasing of the transverse energy is scaled with the initial value. This indicates that the work done by the pressure is also scaled with the initial pressure when it is built up due to thermalization. When looking at the time evolution of collision rate per particle, depicted in Fig. 2 for all scattering channels, we see that the rates are in the same range at late times. This seems to be the reason for the scaling behavior observed for $dE_T/dy|_{y=0}(t)$, since the total collision number per unit time, which corresponds to the work done by the pressure, is proportional to the present local gluon density which is not very different from the initial value for the cases at $p_0 = 1.3 - 1.5$ GeV, seen in Table 1. On the other hand one should realize that small angle scatterings do not really contribute much to (quasi)hydrodynamical work. *Transport* cross sections, or better, *transport* mean free path should and will be discussed in detail within the parton transport approach in future investigations.

In Fig. 1 we also depict the normalized transverse energy per unit rapidity for an ideal hydrodynamical expansion by the thin solid line. Comparisons show that the collective expansion due to the pQCD interactions is quasi ideal at 0.5 – 2 fm/c. At late times the decrease of $dE_T/dy|_{y=0}$ slows down, since the collision rates become smaller, especially in the outer, transversally expanding region where the gluon density is smaller compared to the central region.

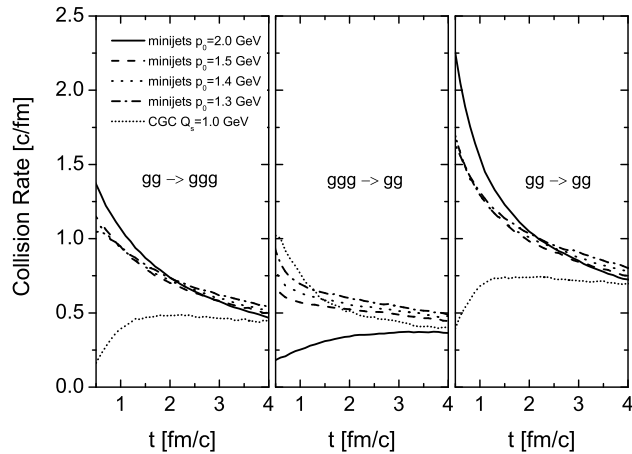


Fig. 2. Time evolution of collision rate extracted in the central region taken as an expanding cylinder with a radius of 1.5 fm and within a unit interval of space time rapidity η around the collision center $\eta = 0$.

Inspecting Fig. 2 again and focusing on the cases at $p_0 = 1.3 - 1.5$ GeV one finds that, at a certain time, the smaller p_0 is, the larger are the rates. This is consistent with the finding shown in Fig. 11 in [1] that at equilibrium the collision rate is proportional to temperature T which is larger in denser system initialized at smaller p_0 . The cross section is then approximately inverse proportional to T^2 . Therefore, at a certain time, the cross sections $\sigma_{gg \rightarrow gg}$ for $gg \rightarrow gg$ and $\sigma_{gg \rightarrow ggg}$ for $gg \rightarrow ggg$ scatterings are smaller at smaller p_0 . For instance, comparing with the time evolution of cross sections calculated at $p_0 = 2.0$ GeV, $\sigma_{gg \rightarrow gg}(\sigma_{gg \rightarrow ggg})$ obtained from the simulation at $p_0 = 1.4$ GeV increases from 0.5(0.3) mb at 0.5 fm/c to 2.5(1.4) mb at 4 fm/c respectively. The values at the final time are approximately 1.6 times smaller than those at $p_0 = 2.0$ GeV, which is consistent with the ratio of T^2 at 4 fm/c [$T = 215(262)$ MeV at $p_0 = 2.0(1.4)$ GeV].

Figure 3 shows kinetic and chemical equilibration observed locally in the central region. The kinetic equilibration is characterized by the time evolution of the momentum anisotropy, $\langle p_T^2 \rangle / 2 \langle p_z^2 \rangle$, which maintains a value of one at equilibrium. For an extreme case of free streaming the final momentum distribution of particles in a local disc would be transversely directed, which leads to an infinite value of the momentum anisotropy. Therefore initial free streaming is the reason for the increase of the momentum anisotropy at the beginning of the expansion, seen in Fig. 3 from the simulations with minijets initial conditions. The following bending over signals the onset of equilibration. We also see that full kinetic equilibrium comes slightly sooner, at 1 – 2 fm/c, at smaller p_0 . The timescale tends to saturate at smaller p_0 . For the case using CGC as initial condition, the momenta of gluons are initially directed transversely in local discs according to Eq. (1). Therefore the

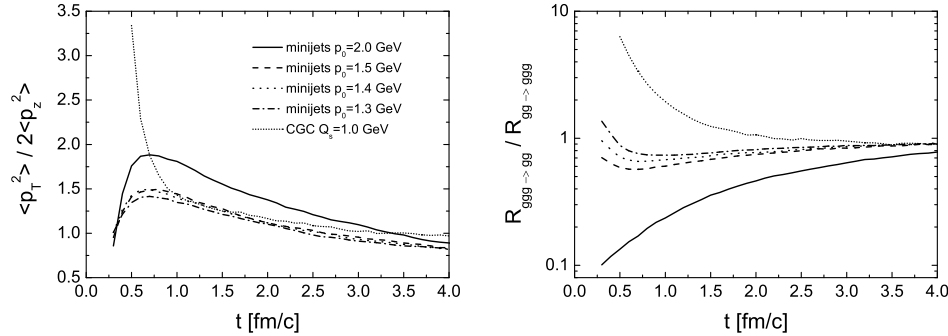


Fig. 3. Left panel: Time evolution of the momentum anisotropy. Right panel: Time evolution of the effective fugacity $\lambda_g = R_{ggg \rightarrow gg}/R_{gg \rightarrow ggg}$. Results are extracted in the central region of the expanding gluon systems simulated using the parton cascade with different initial conditions.

momentum anisotropy has a large initial value. Surprisingly, from 0.8 fm/c the time evolution of the momentum anisotropy is almost identical with that obtained from simulations at smaller p_0 .

In the right panel of Fig. 3 we show the ratio of the collision rates for $ggg \rightarrow gg$ and $gg \rightarrow ggg$ scatterings, which is equal to the gluon fugacity λ_g when the system is at kinetic equilibrium. The collision rates have been already shown in Fig. 2. We realize that the timescale for full chemical equilibrium depends on the initial conditions. At $p_0 = 2.0$ GeV the system is initially undersaturated and reaches full equilibrium at 3 fm/c. At smaller p_0 the system becomes denser and chemical equilibrium is achieved almost initially. For a CGC situation the initial system is oversaturated. Full chemical equilibrium follows at a time ≈ 1.5 fm/c.

Finally, in Fig. 4 we show the transverse momentum spectrum at different times for the case when a color glass condensate is assumed as the initial condition of gluons. We observe that the region around the hard scale $Q_s = 1.0$ GeV, which is mostly populated by initial gluons, is less and less occupied with progressing time. The dominantly populated region moves to smaller p_T scale as cooling proceeds. At 2 fm/c the spectrum possesses a full thermal shape. Thermalization somehow resembles the idealistic bottom-up scenario [9]. However, in clear contrast to that scenario, the gluon number decreases for the particular parameter sets of the initial condition.

5. Conclusion

We have studied local thermalization of gluons in a central Au Au collision at RHIC energy. Initial conditions of gluons are assumed by minijets production at different cutoff $p_0 = 1.3 - 2.0$ GeV and by a color glass condensate with the saturation scale $Q_s = 1.0$ GeV respectively. We apply the newly developed parton cascade including $gg \leftrightarrow ggg$ to simulate the space time evolution of gluons. The numerical results

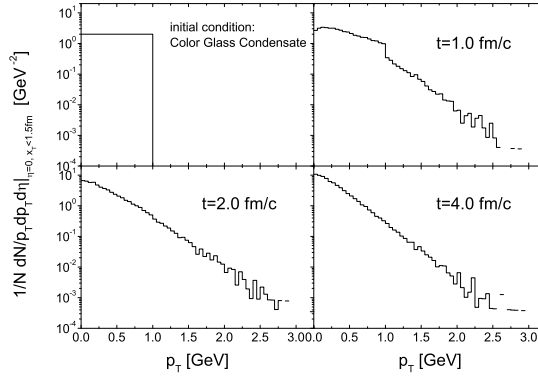


Fig. 4. Transverse momentum spectrum in the central region. Results are obtained from simulation using a color glass condensate as initial condition of gluons.

show that kinetic equilibrium comes sooner in denser system and the timescale tends to saturate, while the dependence of the chemical equilibration on the initial conditions is much stronger.

Future investigations will concentrate on the energy loss of high-energy partons, parametrical dependence of the timescale of thermalization on Q_s and α_s concerning the bottom-up picture, generation of elliptic flow v_2 in noncentral collisions and viscosity in the plasma. Moreover, quarks will be included into the parton cascade. A special interest will be put on the study of elliptic flow of heavy quarks.

References

1. Z. Xu and C. Greiner, *Phys. Rev.* **C71** (2005) 064901.
2. J. Adams et al (STAR Collaboration), *Phys. Rev.* **C70** (2004) 054907.
3. L.D. McLerran and R. Venugopalan, *Phys. Rev.* **D49** (1994) 2233; L.D. McLerran and R. Venugopalan, *ibid.* **49** (1994) 3352.
4. E.J. Eskola, K. Kajantie, P.V. Ruuskanen, and K. Tuominen, *Nucl. Phys.* **B570** (2000) 379; E.J. Eskola, P.V. Ruuskanen, S.S. Räsänen, and K. Tuominen, *Nucl. Phys.* **A696** (2001) 715.
5. M. Glück, E. Reya, and A. Vogt, *Z. Phys.* **C67** (1995) 433.
6. A.H. Mueller, *Nucl. Phys.* **B572** (2000) 227.
7. J. Bitoraker and R. Venugopalan, *Phys. Rev.* **C63** (2001) 024609.
8. T.S. Biro, E. van Doorn, B. Müller, M.H. Thoma, and X.-N. Wang, *Phys. Rev.* **C48** (1993) 1275.
9. R. Baier, A.H. Mueller, D. Schiff, and D.T. Son, *Phys. Lett.* **B502** (2001) 51.